Comparative Study and Survey on the Techniques Employed for Noise Cancellation in CT Images

Jenita Subash

Research Scholar , School of Electronics Engineering, VIT University, Vellore

Dr. S.Kalaivani

Associate Professor

Department of Communication Engineering, School of Electronics Engineering,

VIT University, Vellore, Tamilnadu.

ABSTRACT- It is obligatory to remove high level components of noises in the Medical Images for better diagnosis. There are different medical images for example: Magnetic Resonance Imaging (MRI), X-ray, Computed Tomography and Ultrasound. But the usefulness of all the modalities are invariable degraded by various noises, several noise reduction techniques have been employed for removing these noises.The main aim behind these techniques is to get better results in terms of quality and to speed up the post-processing tasks on the imaging modalities like segmentation, feature extraction etc.,. Several algorithms have been published as of date and each approach has its assumptions, advantages, and limitations. This paper presents comparative study on significant work in the area of image de noising, after conclusion best employed technique will be selected for further work on image de noising.

1. INTRODUCTION

During the past decade, advances in survey and sensor technology have created new opportunities to investigate the structure and dynamics of fluvial systems through the development and differencing of high quality digital terrain models for change detection [1].The numbers of photons emitted from the x-ray tube are characterized as the Poisson distribution this more accurate noise model is justified in multi-energy x-ray CT imaging, where the x-ray energy spectrum is considered. The x-ray energy spectrum can be divided into many sub energy windows (or bins); the number of x-ray photons in each window is Poisson. The mean value of the photons in each energy window can be characterized by a spectrum function $\phi(E)$ [2]. With regard to the repeated CT scans, a previously scanned high-quality diagnostic CT image volume usually contains same anatomical information with the current scan except for some anatomical changes due to internal motion or patient weight change [3].

The metal artefacts actually comprise two main different components. One is photon starvation due to full absorption of x-ray quanta, causing zero-transmission projections. The other is beam hardening due to absorption of low-energy quanta. Although there is no remedy for these artefacts, in clinical practice, higher-energy quanta reduce the extent of artefacts to some degree and could constitute a potential approach to improve diagnostic CT image quality in metallic implants [4].Optical coherence tomography (OCT) generates cross-sectional images by measuring the echo time delay and magnitude of backscattered light.6 Optical coherence tomography has achieved micrometer-level axial resolution in cross-sectional retinal imaging [5].Besides the effect of radiation dose on patients, occupational dose is of major concern. Several cases of lens opacities or cataracts caused by x-ray exposure have been reported. The life time risk of developing cancer, mainly in the left side of the brain, seems to be higher in medical personnel exposed to x-rays [6].

There has been no successful demonstration yet of in vivo XFCT using ordinary X-ray sources. One investigation concluded that XFCT using ordinary sources is not competitive with transmission CT when current clinical scan time and imaging dose constraints are applied to both modalities [7].Most current commercial CT scanners utilize the filtered back projection (FBP) method to analytically reconstruct images. One of the most used methods to reduce the radiation dose is to lower the operating current of the X-ray tube. However, directly lowering the current will significantly degrade the imaging quality due to the excessive quantum noise caused by an insufficient number of photons in the projection domain [8].Using histogram equalization may amplify the noise at the same time. Moreover, for some images with uniformly distributed histogram, the histogram equalization will show limited enhancement of the contrast. The adaptive histogram equalization can enhance the local contrast, which is more robust to the noise than the histogram equalization, and is able to obtain more visually satisfactory results [9].

The usage of dual-energy computed tomography (DECT) in clinical settings is advantageous due to increased tissue discrimination properties obtained from the simultaneous acquisition of two linear attenuation images with different voltage settings [10].

2. LITERATURE SURVEY

(I) Methods Employed

Javerick*et al.*in 2014 [1], had described a six stage methodology involving: i) hand-held image acquisition from

an aerial platform, ii) 3d point cloud extraction modelling using Agisoft Photo Scan, iii) geo-referencing on a redundant network of GPS-surveyed ground-control points, iv) point cloud filtering to reduce computational demand as well as reduce vegetation noise, v) optical bathymetric modelling of inundated areas; and vi) data fusion and surface modeling to generate sub-meter raster terrain models. Bootstrapped geo-registration as well as extensive distributed GPS and sonar based bathymetric check-data were used to quantify the quality of the models generated after each processing step.

Gengsheng*et al.*in 2016[2], started with a hypothetic non-realistic noise model for the CT measurements, by assuming that the attenuation coefficient is energy independent and there is no scattering. A variance formula for this model was derived and presented. Based on that model, computer simulations were conducted with 12 different ad hoc noise weighting methods, and their results are compared.

Zhang*et al.* in 2014 [3], to realize radiation dose reduction by reducing the X-ray tube current and exposure time (mAs) in repeated CT scans, a prior-image induced nonlocal (PINL) regularization for statistical iterative reconstruction via the penalized weighted least-squares (PWLS) criteria had been proposed, which we refer to as "PWLS-PINL".

Kidoh*et al.*in 2014[4], all patients were scanned after contrast material had been delivered over 30 s. The acquisition was performed with Dose Right automatic current selection. CT images were obtained through the oral cavity and neck during the portal venous phase. An automatic bolus-tracking program (Bolus Pro Ultra, Philips Medical Systems) was used to time the start of the scan after contrast medium injection.

YaliJia*et al.* in 2014 [5], Flow was detected using the split-spectrum amplitude de-correlation angiography (SSADA) algorithm. Motion artifacts were removed by 3-dimensional (3D) orthogonal registration and merging of 4 scans. The 3D angiography was segmented into 3 layers: inner retina (to show retinal vasculature), outer retina (to identify CNV), and choroid.

Marco*et al.*in 2015 [6], had proposed two digital subtraction angiography (DSA), One DSA run used standard acquisition chain and image processing algorithms and the other DSA run used dose-reduction and real-time advanced image noise reduction technology. The quality of each pair of runs, consecutively performed without changes in working projection or injection parameters, was independently rated by five radiologists blinded to the imaging technology used. Patient radiation dose was evaluated using air kerma and dose area product, and scatter dose was evaluated using three dosimeters, located at fixed positions.

Moiz*et al.* in 2014 [7], had purposed to increase the sensitivity of XFCT imaging by optimizing the data acquisition geometry for reduced scatter X-rays. The placement of detectors and detector energy window were chosen to minimize scatter X-rays. Both theoretical calculations and Monte Carlo simulations of this optimized detector configuration on a mouse-sized phantom containing various gold concentrations was performed.

Chenn*et al.*in 2016 [8], had described a noise reduction method for low-dose CT via deep learning without accessing the original projection data. Architecture of deep convolution neural network was considered to map the low-dose CT images into its corresponding normal-dose CT images patch by patch.

Huang *et al.*in 2016 [9], had described a method in which, an algorithm including two-stage filtering and contrast enhancement for X-ray images. By using adaptive median filter and bilateral filter, method was able to suppress the mixed noise which contains Gaussian noise and impulsive noise, while preserving the important structures (e.g., edges) in the images. Afterwards, the contrast of image was enhanced by using gray-level morphology and contrast limited histogram equalization (CLAHE).

Rafael *et al.* in 2016 [10], an adaptive neighbourhood Wiener (ANW) filter was implemented and customized to use local characteristics of material density images. The ANW filter employs a three-level wavelet approach, combined with the application of an anisotropic diffusion filter. Material density images and virtual monochromatic images are noise corrected with two resulting noise maps.

(II) Filtering Techniques

Javerick*et al.*in 2014[1], A quality assessment of the workflow combination utilizing SfM, ToPCAT point cloud filtering-point cloud filtering to reduce computational demand as well as reduce vegetation noise. The original SfM–DMVR raw point cloud was filtered in ToPCAT to produce decimated point clouds with 0.75, 1, 2, and 3 m point spacing.

Gengsheng*et al.*in 2016[2], Method number 12 was a practical method that used a low pass filtered version of the measurement to reduce the noise in the weighting function. The filter was a 5-point running average of the noisy data. It was pointed out that the smoothed data were only used for forming the weighting and projection functions to un-smoothed.

Zhang *et al.*in 2014[3], The CT image reconstructed by the FBP method with an optimized Hamming filter from the sinogram data acquired at 100 mAs, 120 kVp. The deformed images were registered to the images reconstructed by the FBP method from the sinogram data acquired at 17 and 40 mAs, respectively.

Kidoh*et al.*in 2014[4], Different approaches towards metal artefact reduction (MAR) have been described, including physical pre-filtering, water correction, and dual energy scanning. The images were reconstructed using a standard filtered back projection (FBP) algorithm with a standard soft-tissue kernel (kernel B; uncorrected image).

YaliJia*et al.*in 2014 [5], to remove flow projection artifacts from superficial retinal blood vessels to the outer retina, firstly a binary large inner retinal vessel map by applying a 30X30 pixel Gaussian filter was generated. This filter removed small inner retinal vessels and masked the outer retina flow map, thus enabling the subtraction of large vessel projections.

Marco*et al.*in 2015 [6], the dose reduction was realized by anatomy specific optimization of the full acquisition chain (grid switch, beam filtering, pulse width, spot size, detector, and image processing engine) for every clinical area. The noise reduction technology combines a spatial and a temporal filter with automatic real-time motion Compensation in subtraction imaging Spatial and temporal filters demonstrate the predominant structures to maintain in the image and smooth out the featureless parts, whereas real-time motion compensation reduces, without any user interaction, the an atomic structure noise introduced by patient movement during subtraction imaging.

Moiz*et al.*in 2014[7], a Hamming filter with a cut-off frequency of $0.25 \times f_{Nq}$ was used for smoothing in the reconstruction; f_{Nq} refers to the Nyquist frequency (is one-half of the sampling frequency). The reconstructed images were assessed using the measured SNR metric:

$$SNR = \frac{\mu_a - \mu_b}{\sigma} \qquad (1)$$

Where, μ_a and μ_b are the mean pixel values in two regions of interest (ROI) *A* and *B*. σ is the standard deviation of pixel values in region *B*. ROI *A* was drawn in a region containing gold solution and *B* was drawn in the water background region in the center of the FOV.

Chen*et al.*in 2016 [8], in the second layer, n_1-dimensional vectors are transformed into n_2 - dimensional ones. This operation was equivalent to a filtration on the feature map from the first layer. The second layer to implement non-linear filtering can be formulated a

$$C_2(Y) = \mathrm{Re}\, LU(W_2 \times C_1(Y) + b_2 \quad (2)$$

Where,

W_2 is composed of n_2 convolution kernels with a uniform size $S_2 \times S_2$ and b_2 has the same size as that of $W_2 \times C_1(Y)$.

Rafael*et al.*in 2016 [10], this technique takes into consideration both single- and dual-source scanners. It employs an adaptive neighbourhood Wiener (ANW) filter to eliminate the noise in the material density images. The resulting noise maps can then be employed to correct the virtual monochromatic images at any energy level.

Image Enhancement implies to rectifying the image from the noise added to it. Couples of filters are required to be done to enhance the quality of the image. Different image enhancement techniques have been studied and presented. De-noising is the process of extraction of added noise from the captured image, to offer better diagnosis. There are various types of noises; some of them are given below.

Gaussian Noise : Gaussian noise is statistical noise that has its probability density function equal to that of the normal distribution, which is also known as the Gaussian distribution.

Impulse Noise: Impulse noise is a category of (acoustic) noise which includes unwanted, almost instantaneous sharp sounds. Noises of the kind are usually caused by electromagnetic interference, scratches on the recording disks and ill synchronization in digital recording and communication

Poison Noise: Poison noise is induced by the nonlinear response of the image detectors and recorders. This type of noise is image data dependent.

2.1. The Generalized flow for de noising the medical images

Salt and Pepper Noise: Salt and pepper noise is a form of noise typically seen on images. It represents itself as randomly occurring white and black pixels.

Speckle Noise: Speckle is a complex phenomenon, which degrades image quality with a backscattered wave appearance which originates from many microscopic diffused reflections that pass through internal organs and makes it more difficult for the observer to discriminate fine detail of the images in diagnostic examinations.

By nature Images contain some amount of noise due to imperfections. But it's difficult to de-noise, So blind de-convolution is employed. Simulated noise is added to the image just to understand the process of de-noising. Because after the addition of mentioned noises if any other transformation or processing is done to the image then the corresponding noises will also be changed. There you will face difficulties to de-noise if you don't know the type of noise. So a known noise is added to the image before processing. So,it is usually employed to test the algorithms or techniques to check how good they are in de-noising process.
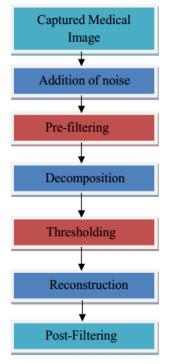

Fig 1: Generalized flow for denoising

Filters: The main function of filters is to suppress either the high frequencies in the image, that is smoothing the image, or the low frequencies, that is enhancing or detecting edges in the image. A digital filter is a system that performs mathematical operations on a sampled, discrete-time signal to reduce or enhance certain aspects of that signal.

Thresholding: The simplest method of image de noising is thresholding. It can be used to create binary image from gray scale image. In thresholding an image is segmented by setting all pixels whose intensity values are above a threshold to a foreground value and all the remaining pixels to a background value.

Comparison Table

1	Javernick et al. in 2014	Modelling the topography of shallow braided rivers using Structure From Motion photogrammetric	A detailed error analysis of sub-meter resolution terrain models of two contiguous Reaches of the braided River generated using SFM.	Simple approach had been employed to cover up couple of problems.	The results are appreciated but have not achieved much superiority than existing approaches	Root mean square error, Mean error,(measure of average non-directional height differences, MAE, standard deviation error
2	Gengsheng et al. in 2016	Does Noise Weighting Matter in CT Iterative Reconstruction	A hypothetic non-realistic noise model for the CT measurements was started, by assuming that the attenuation coefficient is energy independent and there is no scattering. A variance formula for this model was derived and presented	It was reasonable to approximate the more accurate noise model by the less accurate Poisson model and another observation was that the use of the one-time measurement to approximate the mean value of the measurement	Less parameter had been used for the comparison with the other existing techniques.	Variance, contrast, noise standard deviation,
3	Hua Zhang et al. in 2014	Iterative Reconstruction for X-Ray Computed Tomography Using Prior-Image Induced Nonlocal Regularization	To realize radiation dose reduction by reducing the X-ray tube current and exposure time (mAs) in repeated CT scans.	Improved current low-dose image quality.	More number of techniques had been employed for proposed objective.	universal quality index (UQI), contrast-to-noise ratio (CNR), ISNR, rRMSE
7	Moiz Ahmad et al. in 2014	Order of Magnitude Sensitivity Increase in X-ray Fluorescence Computed Tomography (XFCT) Imaging With an	The sensitivity of XFCT imaging can be enhanced by an order of magnitude with the data acquisition optimization, greatly enhancing the potential of this modality for future use in clinical	Improvement in the sensitivity of XFCT by minimizing the acquisition of unwanted scatter X-rays	Only sensitivity factor had been kept in consideration,	SNR,X-ray dose, X-ray source Spectrum,

		Optimized Spectro-Spatial Detector Configuration: Theory and Simulation	molecular imaging.			
11	Ren-You Huang *et al.* in 2014	Noise Removal and contrast enhancement for x-ray images.	The proposed method is able to suppress the mixed noise, which contains Gaussian noise and impulsive noise.	Computational cost has been reduced by detecting corrupted pixels and then median filter is imposed only on them.	Adaptive median filter has slow convergence.	Spiral pattern, angular velocity of spiral, Pitch, spiral curve crosses
12	Rui Song *et al.* in 2015	Improved Goldstein SAR Interferogram Filter Based on Adaptive-Neighbourhood Technique	A modified Goldstein filter based on the adaptive-neighbourhood technique had proposed to filter each pixel of the interferogram within an adjusted filter patch.	The difficulty of estimating the noise level near the borders of different features can be decreased using filtering method.	These methods may result in loss of fine details in an interferogram, especially in areas with dense fringes and complex textures.	Mean coherence, b residues, phase standard deviation, wrapped phase.
13	Julia Stehli *et al.* in 2014	Accuracy of Coronary CT Angiography Using a Fraction of Radiation Exposure	To assess the diagnostic accuracy of CTA acquired with a fraction of effective radiation dose reconstructed with a model-based iterative reconstruction using invasive coronary angiography	Ultra-low-dose contrast enhanced CTA had been used for hypersensitivity to iodinated contrast agent, renal insufficiency non-sinus rhythm, or hemodynamic instability	Large-scale validation should preferably be achieved by multicenter and multivendor studies to establish the robustness of this CTA strategy	BMI (body mass index), tube current mA, tube voltage kV.
14	HolgerHaubenr-eisser*et al.* in 2014	Feasibility of slice width reduction for spiral cranial computed tomography using iterative image reconstruction	prospectively compare image quality of cranial computed tomography (CCT) examinations with varying slice widths using traditional filtered back projection (FBP) versus sinogram-affirmed iterative image reconstruction (SAFIRE)	Improvements in image noise and subjective image quality and image reconstruction.	Only objective and subjective image quality had been considered rather than the effect of reconstruction method and slice thickness on diagnostic accuracy.	fil-tered back projection (FBP), Iterative Reconstruction (IR) for contrast enhamnced and non-contrast enhanced . subjective noise, sharpness
15	Kristin Jensen *et al.* in 2014	Comparing five different iterative reconstruction	to evaluate lesion conspicuity achieved with five different iterative	improve -ment in lesion detection at low	Results do not show how sizes among	ReconstructionMethod Tube Voltage(kV)mAs

		algorithms for computed tomography in an ROC study.	reconstruction techniques from four CT vendors at three different dose levels	doses	patients affect lesion conspicuity with the different algorithms	Rotation time (s)Pitch Collimation Reconstructedslicethic kness Reconstructionfilter
16	Daniel M. Schwartz *et al*.in 2014	Phase-Variance Optical Coherence Tomography	Bulk axial motion of the PV-OCT images was calculated and corrected for each transverse location, reducing the phase noise introduced from eye motion	The choriocapillaris was imaged with better resolution of micro vascular detail using PV-OCT	Results had been formulated in less parameter considerations.	subfovealchoroidal neovascularization (CNV), fluorescein angiography (FA)
17	Yoshitake Yamada *et al*.in 2014	Abdominal CT: An intra-individual comparison between virtual monochromatic spectral and polychromatic 120-kVp images obtained during the same examination	VMS images with filtered back projection (VMS-FBP) and adaptive statistical iterative reconstruction (so-called hybrid IR) (VMS-ASIR) (at 70 keV), as well as 120-kVp images with FBP (120-kVp-FBP) and ASIR (120-kVp-ASIR), Were generated from dual-energy and single-energy CT data, respectively.	subjective image quality scores according to the image reconstruction protocols	A comparison of the noise or CNR between the VMS images and the conventional pure 80-kVp or 100-kVp images would be Desirable.	objective image noises, signal-to-noise ratios and contrast-to-noise ratios, noise , sharpness and overall image quality
18	Adrian Sheppard *et al*.in 2014	Techniques in helical scanning, dynamic imaging and image segmentation for improved quantitative analysis with X-ray micro-CT	dynamic tomography algorithms that enable the changes between one moment and the next to be reconstructed from a sparse set of projections, allowing higher speed imaging of time-varying samples had been presented	improvement in data acquisition efficiency when acquiring 4D tomographic "movies" of certain dynamic processes.	ameliorated by the use of high cone-angle helical scanning and phase contrast effects will be prominent at high resolutions	Gaussian mixture model (GMM),watershed region classification (WRC),ICM
19	Hung Nien*et al*.in 2015	Fast X-Ray CT Image Reconstruction Using a Linearized Augmented Lagrangian Method With Ordered Subsets	solving regularized (weighted) least-squares problems using a linearized variant of AL methods that replaces the quadratic AL penalty term in the scaled augmented Lagrangian with its separable quadratic surrogate function, leading to a simpler ordered-subsets (OS) accelerable splitting-based algorithm, OS-LALM.	the more FISTA iterations, the faster convergence rate of the proposed algorithm. the overhead of iterative inner updates is non-negligible	Reconstruction problem had been mitigated to great extend but still need improvement.	RMSD(HU),system matrix, edge-preserving regularization, weighted quadratic data-fitting term,
20	KLINK Thorsten, *et*	Reducing CT radiation dose	images reconstructed using filtered back projection	IR render image	The results has not been proven	IR,FBP,CTDI , mean tube current,

	*al.*in 2014	with iterative reconstruction algorithms: The influence of scan and reconstruction parameters on image quality and CTDIvol	(FBP) and iterative reconstruction (IR) with reduced tube voltage and current have equivalent quality	quality levels comparable to that of FBP reconstructions at lower tube voltage and tube current	by the images or graphs.	
21	Yan Liu *et al.*in 2014	Total Variation-Stokes Strategy for Sparse-View X-ray CT Image Reconstruction	a total variation-stokes-projection onto convex sets (TVS-POCS) reconstruction had been proposed.	TVS model was to retain the continuous property of the image along both the tangent and the normal directions.	Couple of queries are itself mentioned in the paper which need future work.	MSE, Hanning window, intensity, UQI
22	Yang Chen *at al.*in 2014	Artifact Suppressed Dictionary Learning for Low-dose CT Image Processing	orientation and scale information on artifacts is exploited to train artifact atoms, which are then combined with tissue feature atoms to build three discriminative dictionaries.	the same parameter setting could be applicable to LDCT images of other human body targets as far as they follow the same scan protocol	Still couple of works has to be carried out for the overall improvement, which paper has mentioned in its future works.	sparsity level, tolerance, error tolerance, LDCT,
23	Jochen*et al.*in 2014	Influence of iterative image reconstruction on CT-based calcium score measurements	Iterative reconstruction techniques for coronary CT angiography have been introduced as an alternative for traditional filter back projection (FBP) to reduce image noise, allowing improved image quality and a potential for dose reduction.	the Agatston score, mass score and volume score of calcifications were reduced when using IR images	Results are not compared with the range of ASIR, and results are provided for static percentage of ASIR.	Agatston score, volume , mass, BMI, Number of patients and CT values.
24	Claudia Frellesena*et al.*in 2015	Dual-energy CT of the pancreas: improved carcinoma-to-pancreas contrast with a noise-optimized monoenergetic reconstruction algorithm	Images were reconstructed as linearly-blended 120-kV series (M 0.6) and with the standard monoenergetic (sMERA) and the novel monoenergetic algorithm (nMERA) with photon energies of 40, 55, 70 and 80 keV.	Paper was able to overcome the deterioration of CNR caused by increased noise at low simulated energy level	Work lags in finding of any additional lesions in the monoenergetic images and small number of patients with pancreatic adenocarcinoma had been employed in the design.	Rotation time, pitch ,CTDIvol and DLP, CNR, sMERA and nMERA, SNR.

3. PERFORMANCE EVALUATION

In the above two sections, we have presented comparative study of the proposed methods employed for de noising medical images and the filtering techniques for it. In this section, we are going to investigate the thought put of each approach based on their results. The main focus of survey is on the value of signal to noise ratio, if we are able to minimize the noise, certainly SNR will be higher.

Javerick*et al.* [1], had depicted the values of certain parameters like RMSE, ME, MAE, SDE in the tabulation. The approach was good but it lags while comparing the parameter values of proposed technique with the existing ones. The value had been improved but not to an expected extend.

Gengsheng*et al.*[2], had presented contrast and noise standard deviation graph, contrast of the image had been improved but as far as noise deviation is concerned, it takes more time to stabilize to attain accepted values.

Fig 2: Noise standard deviation

The standard deviation is a measure that is employed to quantify the amount of variation of a set of data values. Lower standard deviation indicates that the data points tend to be close to the expected value of the set, while a high standard deviation indicates that the data points are spread out over a wider range of values. In above graph, it can be noted that obtained values are taking more iterations to get the expected values.

Zhang and Wang [3], had presented the signal to noise ratio for different current ratings, it is presented that signal to noise ratio is improved with increased current ratings in the x-ray. The below graph is depicted for 40mAs, which is better as compared to the 17 mAs. But as the current increases magnetic field effects are increased too, which may lead adverse effects for medical imaging.
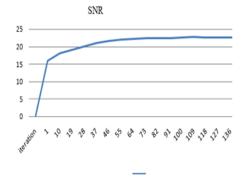

Fig 3: Signal to noise ratio

Signal-to-noise ratio represented as SNR is a measure that compares the level of a desired signal to the level of undesired signal. It is defined as the ratio of signal power to the noise power, often expressed in decibels (dB).

$$SNR = \frac{P_{signal}}{P_{noise}} \quad (3)$$

In figure 3, SNR is depicted with respect to the varying current ratings better results have been achieved for higher currents.

YaliJia*et al.* [5], had presented theoretical discussion for the signal to noise ratio reduction. As investigated the result section seems good and approaching to better throughput, the results lags because of the bluer section at the edges of the scanned images of the retina. Marco [6], had presented DSA performed using a low-dose acquisition chain in combination with advanced real-time image noise reduction technology, in the results section dose reduction is clearly jotted, as far as noise reduction is concerned paper results lags. It can be visualised from the scatter radiation dose images, hue effects can be noted which is the effect of presence of noise,which reduces the image quality

Moiz*et al.*[7], had presented optimization defined with respect to SNR. Although they derived an analytical relationship between SNR and θ in the theoretical model. The detection of the Kβ1 X-rays using θ >110° had been declared the best configuration. SNR was improved in the optimized configuration.

Chen*et al.* [8], had presented the parameters in ASD-POCS, KSVD and BM3D were adjusted to achieve best average PSNR values for different noise levels. BM3D-F indicates running BM3D with fixed parameter for b_0 =10^5.Where b_0 represents the noise level. It can be visualised that all the parameters have attained good improvement in SNR. But still further work can be done on this technique.
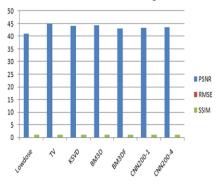

Fig 4: Peak signal to noise ratio

The root-mean-square-error is employed to measure the differences between values predicted by a model and the values actually observed. The RMSE represents the sample standard deviation of the differences between predicted values and observed values.The structural similarity (SSIM) index is used for predicting the perceived quality. SSIM is used for measuring the similarity between two images.The prediction

of image quality is based on an initial distortion-free image as reference. SSIM is outlined to improve traditional methods such as peak signal-to-noise ratio (PSNR) and mean squared error (MSE), which have proven to be inconsistent with human visual perception.

In figure 4, PSNR, RMSE and SSIM parameters has been shown for different techniques. It can be noted that SNR is high for all technique which is the sign of efficient algorithm.

Huang*et al.*[9], had presented tested graph of images with mixed noises. Graph shows the PSNR of the results of different methods. The results in the proposed method had been presented by the combination of adaptive median filer and bilateral filter. The SNR improvement approach was good but the performance of technique is dependable on the filtering techniques, moreover adaptive filter has slow convergence.
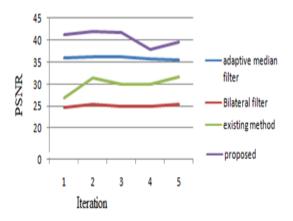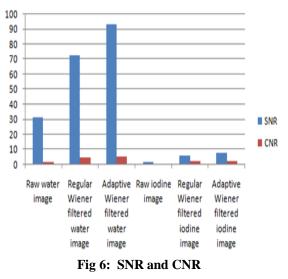

Fig 5: PSNR for mixed noise

Rafael*et al.* [10],had presented behaviour of the algorithm using the adaptive Wiener filter was superior to that of the algorithm with the standard Wiener filter, for both SNR and CNR gains in all three kinds of acquisition techniques selected for the comparison. As per the results SNR has been improved in the range of 60-75%, which can be considered good. But still work need to carryout to satisfactory level.

Fig 6: SNR and CNR

In figure 6, affectiveness of the algorithm has been checked with different filtering techniques. It can be noted that adaptive wiener filter has shown better results for SNR and CNR.

The results of few researches are depicted in the form of graphs, which are implemented by their techniques separately and results are compared visually on the basis of quantitative analysis. The technique having better results will be taken to next level by clubbing with some advanced and efficient techniques.

4. CONCLUSION

It is necessary to remove the noise content from the medical images to a great extend to achieve better diagnosis.The comparison table is survey, which can be helpful for the researches by having consequences of each technique and proceed with the advantageous factors of certain techniques to propose better de-noising technique. In this paper we went through an investigation process, to find the techniques which had been employed for de noising process and further which one of them yields better throughput. After going through all the process of survey, on the basis of quantitative analysis, we conclude that, Neural network can able to enhance the sensitive regions with higher visual quality.

REFERENCES

[1] L. Javernick, J. Brasington and B. Caruso, "Modeling the topography of shallow braided rivers using Structure-from-Motion photogrammetry", Elsevier, Vol. 213, Pages 166 - 182, May 2014.

[2] Gengsheng. L. Zeng and Wenli Wang, "Does Noise Weighting Matter in CT Iterative Reconstruction?",IEEE Transactions on Nuclear Science, Vol. PP, Issue No. 99, November 2016.

[3]Hua Zhang, Jing Huang, Jianhua Ma, ZhaoyingBian, QianjinFeng, Hongbing Lu, Zhengrong Liang, and Wufan Chen, "Iterative Reconstruction for X-Ray Computed Tomography Using Prior-Image Induced Nonlocal Regularization", IEEE Transactions on Biomedical Engineering, Vol. 61, Issue No. 9, SEPTEMBER 2014

[4] M. Kidoh, T. Nakaura, S. Nakamura, S. Tokuyasu, H. Osakabe, K. Harada, Y. Yamashita, "Reduction of dental metallic artefacts in CT: Value of a newly developed algorithm for metal artefact reduction (O-MAR)", Elsevier, Volume 69, Issue 1, January 2014.

[5] YaliJia, Steven T. Bailey, David J. Wilson, Ou Tan, Michael L. Klein, MD, Christina J. Flaxel, Benjamin Potsaid, Jonathan J. Liu, Chen D. Lu, Martin F. Kraus,James G. Fujimoto and David Huang, "Quantitative Optical Coherence Tomography Angiography of Choroidal Neovascularization in Age-related Macular Degeneration", Elsevier, Volume 121(7), pages 1435-44, March 2014.

[6]Marco J. Van Strijen, ThijsGrünhagen, Maria Mauti, Markus Zähringer, Peter A. Gaines, Graham J. Robinson, Nicholas J. Railton, Hans van Overhagen, Jan Habraken and Marc van Leersum, "Evaluation of a Noise Reduction Imaging Technology in Iliac Digital Subtraction Angiography: Noninferior Clinical Image Quality with Lower Patient and ScatterDose", Elsevier, Volume 26(5), Pages 642-50, May 2015.

[7] Moiz Ahmad, Magdalena Bazalova, Liangzhong Xiang, and Lei Xing, "Order of Magnitude Sensitivity Increase in X-ray Fluorescence Computed Tomography (XFCT) Imaging With an Optimized Spectro-Spatial Detector Configuration: Theory and Simulation", IEEE Transactions on Medical imaging, Volume No. 33,Issur No. 5, MAY 2014.

[8] Hu Chen, Yi Zhang, Weihua Zhang, Peixi Liao, Ke Li1, Jiliu Zhou and Ge Wang, "Low-Dose CT via Deep Neural Network", arXiv, Issue No 1609.0850, September 2016.

[9]Ren-You Huang, Lan-Rong Dung, Cheng-Fa Chu and Yin-Yi Wu, "Noise removal and contrast enhancement for X-ray Images", Journal of Biomedical Engineering and Medical Imaging, Volume 3, No 1, pp 56-67, February 2016.

[10]Rafael Simon Maia, Christian Jacob, Amy K. Hara, Alvin C. Silva, William Pavlicek, J. Ross Mitchell, "Adaptive noise correction of dual-energy computed tomography images", Springer link, Volume No. 11(4), Page No. 667-78, April 2016.

[11] M. S. Rana, H. R. Pota and I. R. Petersen, "Spiral Scanning With Improved Control for Faster Imaging of AFM", IEEE Transactions on Nanotechnology, Volume No. 13, Issue No. 3, May 2014.

[12] Rui Song, HuadongGuo, Guang Liu, ZbigniewPerski, HuanyinYue, Chunming Han, and Jinghui Fan, "Improved Goldstein SAR Interferogram Filter Based on Adaptive Neighborhood Technique", IEEE Geoscience and Remote Sensing Letters, Volume No. 12, Issue No. 1, January 2015.

[13]Julia Stehli, Tobias A. Fuchs, Sacha Bull, Olivier F. Clerc, Mathias Possner, Ronny R. Buechel, Oliver Gaemperli, Philipp A. Kaufmann, "Accuracy of Coronary CT Angiography Using a Submillisievert Fraction of Radiation Exposure", Elsevier, Volume No. 64, Issue No. 8, August 2014.

[14] HolgerHaubenreisser, Christian Fink, John W. Nance Jr, Martin Sedlmair, Bernhard Schmidt, Stefan O. Schoenberg, Thomas Henzler, "Feasibility of slice width reduction for spiral cranial computed tomography using iterative image reconstruction", Elsevier, Volume No. 83, PP 964-969, January 2014.

[15] Kristin Jensen, Anne Catrine T. Martinsen, Anders Tingberg, TrondMogensAaløkken and Erik Fosse, "Comparing five different iterative reconstruction algorithms for computed tomography in an ROC study", Springer, Volume No. 24, Issue No. 12,December 2014.

[16] Daniel M. Schwartz, Jeff Fingler,Dae Yu Kim, Robert J. Zawadzki, Lawrence S. Morse, Susanna S. Park, Scott E. Fraser, John S. Werner, "Phase-Variance Optical Coherence Tomography", Elsevier, Volume No. 121, Issue No 1, January 2014.

[17] Yoshitake Yamada, Masahiro Jinzaki, Takahiro Hosokawa, Yutaka Tanami, Takayuki Abe, Sachio Kuribayashi, "Abdominal CT: An intra-individual comparison between virtual monochromatic spectral and polychromatic 120-kVp images obtained during the same examination", Elsevier, Volume No. 83, Issue No. 10, October 2014.

[18]Adrian Sheppard, Shane Latham, Jill Middleton, Andrew Kingston, Glenn Myers, TrondVarslot, Andrew Fogden, Tim Sawkins, Ron Cruikshank, Mohammad Saadatfar1, Nicolas Francois, ChristophArns and Tim Senden, "Techniques in helical scanning, dynamic imaging and image segmentation for improved quantitative analysis with X-ray micro-CT", Elservier, Volume No. 324, Pages 49-56, April 2014.

[19] Hung Nien and Jeffrey A. Fessler, "Fast X-Ray CT Image Reconstruction Using a Linearized Augmented Lagrangian Method With Ordered Subsets", IEEE Transactions on Medical Imaging, Vol. 34, no. 2, February 2015.

[20]Klink Thorsten, Ebcr, Obmann Verena C, Heverhagen Johannes, Stork Alexander, ADAM Gerhard and BEGEMANN Philipp G, "Reducing CT radiation dose with iterative reconstruction algorithms: The influence of scan and reconstruction parameters on image quality and CTDI", Elsevier, Volume No. 83, Issue No. 9, September 2014.

[21] Yan Liu, Zhengrong Liang, Jianhua Ma, Hongbing Lu, Ke Wang, Hao Zhang, and William Moore, "Total Variation-Stokes Strategy for Sparse-View X-ray CT Image Reconstruction", IEEE Transactions on Medical Imaging, Vol. No. 33, Issue No. 3, march 2014.

[22] Yang Chen, Luyao Shi, QianjingFeng, Jiang Yang, HuazhongShu, LiminLuo, Jean-Louis Coatrieux and Wufan Chen, "Artifact Suppressed Dictionary Learning for Low-Dose CT Image ProcessingArtifact Suppressed Dictionary Learning for Low-Dose CT Image Processing", IEEE Transactions on Medical Imaging, Volume No. 33, Issue No. 12, 2014.

[23] Jochen A. C. van Osch, Mohamed Mouden, Jorn A. van Dalen ,Jorik R. Timmer, StofferReiffers, SiertKnollema, Marcel J. W. Greuter, Jan Paul Ottervanger and Piet L. Jager, "Influence of iterative image reconstruction on CT-based calcium score measurements", Springer, Volume No 30, issue No 5, 2014.

[24]Claudia Frellesen, FreiaFessler, Andrew D. Hardie, Julian L. Wichmann, Carlo N. De Cecco, U. Joseph Schoepf, J. Matthias Kerl, Boris Schulz,RenateHammerstingl, Thomas J. Vogl, Ralf W. Bauer, "Dual-energy CT of the pancreas: improved carcinoma-to-pancreas contrast with a noise-optimized monoenergetic reconstruction algorithm", Elsevier, Volume No. 84, Pages 2052-2058, 2015.